arXiv:1211.1012v1 [astro-ph.CO] 5 Nov 2012

Linear dark energy equation of state revealed by supernovae?

Vincenzo Salzano[1], Yun Wang[2], Irene Sendra[1], and Ruth Lazkoz[1]
[1]*Fisika Teorikoaren eta Zientziaren Historia Saila, Zientzia eta Teknologia Fakultatea,*
Euskal Herriko Unibertsitatea, 644 Posta Kutxatila, 48080 Bilbao, Spain and
[2]*Homer L. Dodge Department of Physics & Astronomy,*
Univ. of Oklahoma, 440 W Brooks St., Norman, OK 73019, U.S.A.
(Dated: November 7, 2012)

In this letter we propose a test to detect the linearity of the dark energy equation of state, and apply it to two different Type Ia Supernova (SN Ia) data sets, Union2.1 and SNLS3. We find that: *a.* current SN Ia data are well described by a dark energy equation of state linear in the cosmic scale factor a, at least up to a redshift $z = 1$, independent of the pivot points chosen for the linear relation; *b.* there is no significant evidence of any deviation from linearity. This apparent linearity may reflect the limit of dark energy information extractable from current SN Ia data.

PACS numbers: $95.36.+x, 98.80.Es, 98.80.-k, 97.60.Bw$
Keywords: Cosmology, Dark Energy, Supernovae.

Introduction - After the discovery of the accelerated expansion of our Universe [1], many models have been proposed to solve the mystery of dark energy, both in the context of general relativity and of alternative gravity theories [2]. Models are characterized by an analytical expression for the dark energy equation of state (EoS), derived either by phenomenological or theoretical considerations; and generally depending on two or more parameters [3] which can be constrained using observations. A very short, not exhaustive, summary of the most used EoS parameterizations is in [4, 5]; among them, the CPL model [4] is considered as the reference model. It is defined as $w(a) = w_0 + (1-a)w_a$: w_0 is the EoS present value ($a = 1$ or $z = 0$) and $w_\infty = w_0 + w_a$ is the asymptotic value of EoS at early times ($a \to 0$ or $z \to \infty$). This model has some well known problems: the high correlation between its two parameters, and the high-redshift dependence of the parameter w_a, which makes its use with low-redshift limited data questionable. An alternative parametrization is *Wang's model* [6]:

$$w(a) = \left(\frac{a_c - a}{a_c - 1}\right) w_0 + \left(\frac{a-1}{a_c-1}\right) w_c \,, \qquad (1)$$

where $w_c = w(a_c)$ is the EoS calculated at the pivot value for the cosmic scale factor a, chosen to minimize the correlation between the EoS parameters, w_0 and w_c. In a broader view, we can see that Wang's model is a linear interpolation between two points, $(a_1, w_1 = w(a_1))$ and $(a_2, w_2 = w(a_2))$; thus we can define a *General Linear EoS model* (GL) by

$$w(a) = \left(\frac{a_2 - a}{a_2 - a_1}\right) w_1 + \left(\frac{a_1 - a}{a_1 - a_2}\right) w_2 \,. \qquad (2)$$

We obtain Eq. (1) if $a_1 = a_0 = 1$ and $a_2 = a_c$.

GL models can be used to test whether the dark energy EoS is *linear or not* in the scale factor. This test has nontrivial implications: if linearity is verified, all models in [5] deviating from it may be discarded. If the EoS is not effectively linear, then the CPL model is *intrinsically wrong.* To test this possibility in the most general way, we can generalize the GL model to higher-order polynomial functions; an interpolation function between $\mathcal{N}$ points can be written in a general fashion as:

$$w_a = \sum_{i=1}^{\mathcal{N}} w_i \left(\prod_{j \neq i}^{\mathcal{N}} \frac{a_j - a}{a_j - a_i} \right) \qquad (3)$$

with $\mathcal{N} = 2$ for the GL model; $\mathcal{N} = 3$ for a *second-order interpolation model* ($2NL$); $\mathcal{N} = 4$ for a *third-order interpolation model* ($3NL$); and so on. A third possibility is that current SNeIa data do not allow us to distinguish between a linear and a nonlinear EoS, and linearity could be an *artifact* coming from the data used.

This test can be implemented very easily, as illustrated in Fig. 1. Let us suppose to have an exact EoS whose (unknown) profile is the solid line in the figure; the dots are the pivot values where the GL EoS is to be calculated; the dashed lines represent the GL models (linear interpolations) using different pairs of pivots. If the underlying EoS is not linear (left panel), then we will obtain different estimations of the pivot values when using different GL parameterizations; on the other side, if the EoS is linear (or with a *very small* curvature; right panel), such estimations will yield the same linear relation, independent of the GL model considered.

Data - We will use SNeIa data from two different samples: the Union2.1 compilation [7] and the SNLS3 compilation that includes the three year data from the *SuperNova Legacy Survey* [8]. The χ^2 is generally defined as $\chi^2 = \Delta\boldsymbol{\mathcal{F}} \cdot \mathbf{C}^{-1} \cdot \Delta\boldsymbol{\mathcal{F}}$. $\Delta\boldsymbol{\mathcal{F}} = \mathcal{F}_{theo} - \mathcal{F}_{obs}$ is the difference between the observed and theoretical value of the observable quantity, $\mathcal{F}$; this will be the distance modulus μ for Union2.1 and the SNeIa magnitude m_{mod} for SNLS3:

$$\mu = 5\log_{10}[H_0 d_L(z, \Omega_m; \boldsymbol{\theta})] + \mu_0 \,; \qquad (4)$$

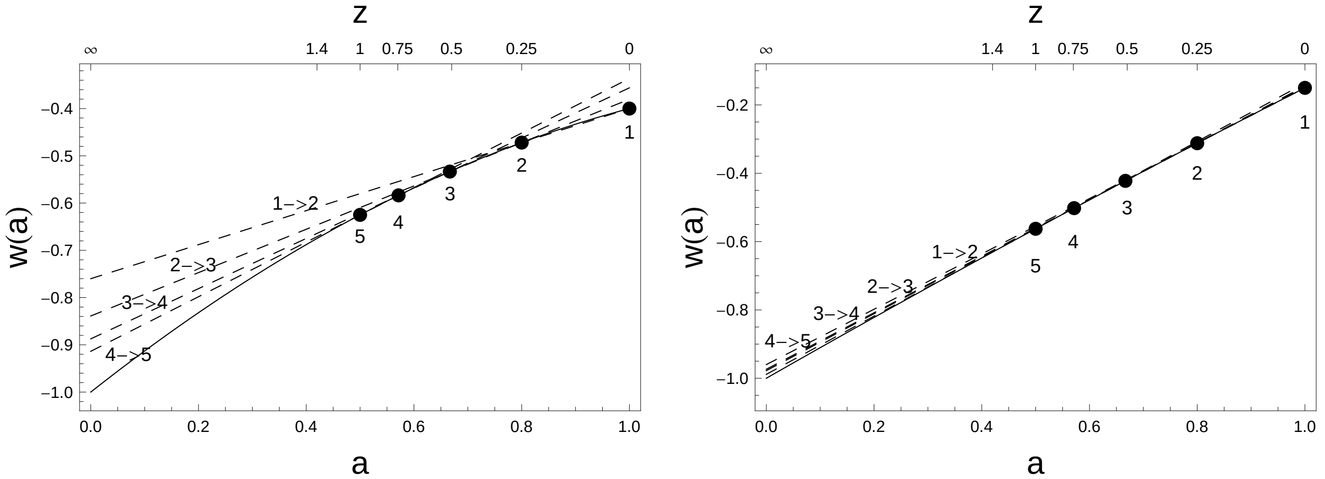

Figure 1. Test of linearity of dark energy EoS through the GL models defined in Eq. (2): solid line is the underlying unknown EoS function which we want to reconstruct; dots are the pivot scale factor values chosen to define various GL models; dashed lines are the GL models calculated varying the pivot values. In the left panel, the underlying EoS is not linear; in the right one, it is almost linear (very small curvature).

$$m_{\rm mod} = 5\log_{10}[H_0 d_L(z,\Omega_m;\boldsymbol{\theta})] - \alpha(s-1) + \beta\mathcal{C} + \mathcal{M} \; . \quad (5)$$

Note that

$$H_0 d_L(z,\Omega_m;\boldsymbol{\theta}) = (1+z)\int_0^z \frac{{\rm d}z'}{E(z',\Omega_m;\boldsymbol{\theta})} \, , \quad (6)$$

$$E(z) = \frac{H(z)}{H_0} = \left[\Omega_m(1+z)^3 + (1-\Omega_m)X(z,\boldsymbol{\theta})\right]^{1/2} \, , \quad (7)$$

$$X(z,\boldsymbol{\theta}) = \exp\left[3\int_a^1 \frac{da'}{a'}(1+w(a',\boldsymbol{\theta}))\right] \, . \quad (8)$$

with $\boldsymbol{\theta}$ the dark energy EoS parameters vector ($\boldsymbol{\theta} = (w_1, w_2)$ for GL models).

The matter content will be fixed as $\Omega_m = 0.259$[1] [9]; μ_0 and $\mathcal{M}$ are nuisance parameters combining the Hubble constant H_0 and the absolute magnitude of a fiducial SN Ia, and we minimized χ^2 (through a Monte Carlo Markov Chain (MCMC) algorithm) by marginalizing over them [8]. Finally, $\mathbf{C}$ is the covariance matrix: in the SNLS3 case, it depends on the parameters α and β, considered as free fitting parameters; in the Union2.1 case they are fixed. For a more detailed discussion about the difference between the two approaches, we refer to [8]. To test each model, we calculate the Bayesian evidence, defined as the probability of the data D given the model M with a set of parameters $\boldsymbol{\theta}$, $\mathcal{E}(M) = \int {\rm d}\boldsymbol{\theta} L(D|\boldsymbol{\theta}, M)\pi(\boldsymbol{\theta}|M)$: $\pi(\boldsymbol{\theta}|M)$ is the prior on the set of parameters, normalized to unity, and $L(D|\boldsymbol{\theta}, M)$ is the likelihood function. The evidence is estimated using the algorithm in [10]. To reduce the statistical noise we run the algorithm many times obtaining a distribution of ~ 1000 values from which we extract the best value of the evidence as the mean of such distribution. Then, we calculate the Bayes Factor, defined as the ratio of evidences of two models, M_i and M_j, $\mathcal{B}_{ij} = \mathcal{E}_i/\mathcal{E}_j$. If $\mathcal{B}_{ij} > 1$, model M_i is preferred over M_j, given the data. The Bayesian evidence is interpreted using Jeffreys' Scale: if $\ln\mathcal{B}_{ij} < 1$ there is not significant preference for the model with the highest evidence; if $1 < \ln\mathcal{B}_{ij} < 2.5$ the preference is substantial; if $2.5 < \ln\mathcal{B}_{ij} < 5$ it is strong; if $\ln\mathcal{B}_{ij} > 5$ it is decisive. We will use the $(0-0.5)$ GL model as reference model i.

Results - First we focus on the information that can be extracted using different GL models. Final results are summarized in Table I. We have chosen 5 pivot values for the scale factor, equally spaced in the redshift space (an arbitrary choice which has no effect on final results) and up to a maximum redshift $z = 1$ (the redshift value where the SNeIa number density is statistically significant). They are $z = \{0, 0.25, 0.5, 0.75, 1\}$ (corresponding to scale factors $a = \{1, 0.8, 0.67, 0.57, 0.5\}$). For each GL parametrization we have two primary parameters (bold text in tables), namely, the EoS calculated at the pivot redshifts and directly derived as fitting parameters; and secondary parameters (plain text), the EoS calculated in the remaining chosen pivot values and derived from the obtained best GL EoS relation. We also perform fits with a cosmological constant and the CPL model for comparison.

We find the following about the absolute value of the EoS parameters:

---

[1] We fix the value of Ω_m in order to reduce the degeneracy between cosmological parameters and EoS dark energy parameters (w_0, w_a). We have explored also the case of $\Omega_m = 0.271$ and Ω_m free. We omit the description of such results: we have a small shift in the absolute values of the cosmological parameters in question and, when Ω_m is free, somewhat larger errors on them, but our conclusions are not changed at all.

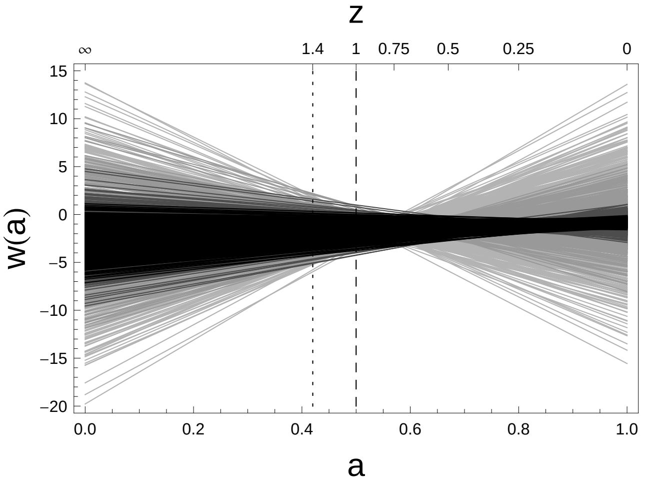

Figure 2. Summary of all GL models: SNLS3 sample joining al the GL models in Table. I.

- the primary EoS parameters are almost perfectly consistent with each other, independent of the GL model considered. We note that, given the nature of the MCMC algorithm, there is an intrinsic statistical background noise (i.e. nonphysically meaningful fluctuations) to be considered;

- the same good agreement is valid for secondary parameters; particularly impressive is the consistency with the $w_\infty = w_0 + w_a$ derived from the CPL model.

These are two strong points in favor of a linear (in scale factor) parametrization for the dark energy EoS, *at least up to* $z = 1$. Of course, we have to compare such results with the errors on these parameters:

- we join all GL models: for each GL parametrization, we randomly extract $N = 1000$ pairs of pivot EoS parameters, (w_1, w_2), from Gaussian distributions centered on the best fit values from each model and with dispersion equal to the MCMC derived errors; then we plot the resulting GL models in Fig. 2 and we show the total errors on each EoS parameters in the last row of Table I. We see there is a minimum in dark energy EoS parameters error at $z \sim 0.25$; this same value is obtained in [6] as the redshift corresponding to the minimal correlation between the pivot parameters, while errors on w_0 are comparable with errors on $w_{0.75}$;

- the errors generally grow when moving to higher redshift pivot values: this is somewhat expected as, in general the SN Ia number density fades out toward higher redshifts. If we consider 0.1-width redshift bins, the SNLS3 sample has ~ 120 objects at $z < 0.1$ and ≈ 40 objects per bin up to $z \sim 0.9$; this, of course, influences the estimation of the pivot EoS parameters with a degradation of the reconstructed value at higher redshifts;

Finally, we note that the Bayes factor (with the $(0-0.5)$ GL model as reference) is much less than 0.05: GL models are practically equivalent. This is an important consistency check in favor of linearity. But, considering the behavior of the errors, an important question arises: *does the error-redshift relation depend on the number of data points, or is it a signal of an intrinsic breakdown of the linear EoS model?*. As we have shown in the left panel of Fig. 1, a non-linear EoS can produce different estimated values for the pivot parameters *or*, *equivalently*, a wider dispersion, i.e. larger errors on them. In order to check this, we have analyzed the $2NL$ and $3NL$ models, so that we can compare linear models to second and third-order interpolation functions. Results are given in Table. II:

- the primary EoS parameters are not consistent with each other as in the case of GL models; in particular the agreement among the derived w_∞ values goes down;

- errors are much larger than the GL models, due to the larger number of estimated parameters;

- interestingly, even with these models, the $w_{0.25}$ pivot corresponds to the best estimation of the dark energy EoS; this could be a further indication that this depends on the higher number of points at lower redshift more than on intrinsic properties of EoS;

- it is quite puzzling to note the value of the Bayes Factor: it is > 0.4 for the $2NL$ models and > 0.35 for the $3NL$ ones. It is quite larger than the values from the GL models, so that non-linear models are disfavored; but it is also lower than the values which, following the Jeffreys scale, would give strong preference to the linear model.

All the points above lead to the conclusion that a linear EoS for dark energy is the most statistically probable choice when using SNeIa as cosmological tools. The black region in Fig. 2 is the 68% confidence region, the most probable region where $w(a)$ can lie. Clearly the values of the errors, as explained above, still leave open the possibility for non-linear models; probably, with the addition of more SNeIa in the future and at higher redshifts, we will be able to give even stronger constraints to the global EoS trend (presumably reducing the black region in the figure) and we would probably enhance further the evidence for linearity of dark energy EoS.

Nevertheless, we have to consider another possibility. We have also used the Union2.1 sample; results for it are given in Table. III. All the comments we have given for SNLS3 are *qualitatively and globally* true also for the Union2.1 data. In general, Union2.1 data show errors which are always slightly smaller than those from SNLS3, mainly because Union2.1 has more low redshift SNeIa (if we consider 0.1-width redshift bins, we have ~ 100 objects at $z < 0.1$, then we have a peak of ~ 60 objects per bin in $0.1 < z < 0.5$ and ≈ 20 objects per bin in $0.7 < z < 1.0$) which can more tightly constrain the behavior of EoS at higher redshifts. The behavior of the GL models at high redshift is even more interesting; we obtain two completely different asymptotical behaviors: SNLS3 points to a very phantom early dark energy ($w_\infty \approx -2.6$) which implies $w_a < 0$ and $|w_a| > |w_0|$; Union2.1 has less negative EoS ($w_\infty = -0.7$), or equivalently, $w_a > 0$ and $|w_a| < |w_0|$. While flux-averaging [11] may reduce this dramatic difference somewhat, it will likely not remove it, since it most probably originates from the fact that covariance matrices are obtained and handled very differently when obtaining the two data samples. However, both samples are very compatible with a linear EoS.

To conclude, we have found *that current SN Ia data are well described by a dark energy EoS linear in a, independent of the pivot points chosen for the linear relation, and that there is no significant evidence of any deviation from linearity.* This may indicate that the dark energy EoS is a linear function in a, or that current data only allow the extraction of a linear function. Significantly larger SN Ia data sets will be required to clarify this.

Acknowledgments - V.S., I.S. and R.L. are supported by the Spanish Ministry of Economy and Competitiveness through research projects FIS2010-15492 and Consolider EPI CSD2010-00064, by the Basque Government through the special research action KATEA and ETORKOSMO, and by the University of the Basque Country UPV/EHU under program UFI 11/55. I.S. holds a PhD FPI fellowship contract from the mentioned ministry. Y.W. is supported in part by DOE grant DE-FG02-04ER41305.

[1] Riess et al., Astrophys. J 116 (1998) 1009. S. Perlmutter, et al., Astrophys. J. 517 (1999) 565.

[2] D. Sapone, Int. J. Mod. Phys. **A25** (2010) 5253; J. Frieman, M. Turner, D. Huterer, Ann. Rev. Astron. Astrophys. 46 (2008) 385; V. Sahni, A. Starobinsky, Int. J. Mod. Phys. D15 (2006) 2105; S. Tsujikawa, arXiv:1004.1493; Carroll, S.M., Press, W.H., Turner, E.L, ARA&A (1992), 30, 499; Sahni, V., Starobinski, A. 2000, Int. J. Mod. Phys. D, 9, 373; Capozziello, S., 2002, Int. Jou. Mod. Phys., D 11, 483; Capozziello, S. and Francaviglia, M., 2008, Gen. Rel. Grav., 40, 357; E. J. Copeland, M. Sami, S. Tsujikawa, Int. J. Mod. Phys. D15 (2006) 1753; Manera M. & Mota D., 2006, Mon. Not. Roy. Astron. Soc. 371, 1373; Mota D. F., 2008, JCAP 09006; Koivisto T., Mota D. F., Phys. Rev. 2006, D73, 083502; Li B., Barrow J.D., Mota D. F. , 2007, Phys. Rev. D76, 104047; Koivisto, T. S., Mota D. F., Pitrou C., 2009, JHEP 0909, 092; Padmanabhan, T. 2003, Phys. Rep., 380, 235; Peebles, P.J.E., Rathra, B. 2003, Rev. Mod. Phys., 75, 559; Capozziello, S. and De Laurentis, M., 2011, Phys. Repts., 509, 167.

[3] Linder, E. V., Huterer, D., Phys. Rev. D, 72 (2005) 043509; Sarkar, D., Sullivan, S., Joudaki, S., Amblard, A., Holz, D. E., Cooray, A., Phys. Rev. Lett., 100 (2008) 231302.

[4] M. Chevallier, D. Polarski, Int. J. Mod. Phys. D. 10 (2001) 213; E. V. Linder, Phys. Rev. Lett. 90 (2003) 091301;

[5] A. R. Cooray, D. Huterer, Astrophys. J. 513 (1999) L95; F. Efstathiou, Mon. Not. Roy. Astron. Soc. 310 (1999) 842; P. Astier, Phys. Lett. B 500 (2001) 8; M. Goliath, R. Amanullah, P. Astier, A. Goobar, R. Pain, Astron. Astrophys. 380 (2001) 6; J. Weller, A. Albrecht, Phys. Rev. D 65 (2002) 103512; V. Sahni, T. D. Saini, A. A. Starobinsky, U. Alam, JETP Lett. 77 (2003) 201; C. Wetterich, Phys. Lett. B 594 (2004) 17; T. Padmanabhanm, T. R. Choudhury, Mon. Not. Roy. Astron. Soc. 356 (2005) 611 E. M. Barboza, J. S. Alcaniz, B. Santos, arXiv:1107.2628; J. - Z. Ma, X. Zhang, Phys. Lett. B 699 (2011) 233;

[6] Y. Wang, Phys. Rev. D 77 (2008) 123525.

[7] N. Suzuki et al., Astrophys. J. 746 (2012) 85S.

[8] J. Guy, M. Sullivan, A. Conley, et al., Astron. Astrophys. 523 (2010) 7; A. Conley, J. Guy, M. Sullivan, et al., Astrophys. J. Supp. 192 (2011) 1; M. Sullivan, J. Guy, A. Conley, et al., Astrophys. J. 737 (2011)102S.

[9] http://lambda.gsfc.nasa.gov/product/map/current /parameters.cfm

[10] P. Mukherjee, D. Parkinson, A.R. Liddle, Astrophys. J. 638 (2006) 51-51.

[11] Y. Wang, Astrophys. J. 536 (2000) 531; Y. Wang, P. Mukherjee, Astrophys. J. 606 (2004) 654-663; Y. Wang, New. Astron. Rev. 49 (2005) 97-102; Y. Wang, Phys. Rev. D 80 (2009) 123525; Y. Wang, C. H. Chuang, P. Mukherjee, Phys. Rev. D 85 (2012) 023517.

Table I. Linear EoS test with SNLS3 data. For any EoS parametrization (first column) we give primary fitted parameters in bold text and secondary derived parameters in plain text. Errors for the primary parameters are derived directly from the MCMC procedure; the errors on secondary parameters are calculated following the standard error propagation theory.

SNLS3	Ω_m			w (fixed)			α	β	$\ln \mathcal{B}_{ij}$
ΛCDM	$0.228^{+0.039}_{-0.038}$			-1			$1.434^{+0.110}_{-0.105}$	$3.265^{+0.111}_{-0.109}$	0.03
	w_0	$w_{0.25}$	$w_{0.5}$	$w_{0.75}$	w_1	w_∞	α	β	$\ln \mathcal{B}_{ij}$
CPL	$\boldsymbol{-0.826^{+0.199}_{-0.209}}$	$-1.188^{+0.357}_{-0.387}$	$-1.429^{+0.550}_{-0.598}$	$-1.602^{+0.695}_{-0.757}$	$-1.731^{+0.806}_{-0.879}$	$\boldsymbol{-2.636^{+1.600}_{-1.745}}$	$1.435^{+0.110}_{-0.105}$	$3.276^{+0.112}_{-0.110}$	-0.02
$(0-0.25)$	$\boldsymbol{-0.824^{+0.216}_{-0.212}}$	$\boldsymbol{-1.187^{+0.150}_{-0.178}}$	$-1.429^{+0.288}_{-0.329}$	$-1.602^{+0.405}_{-0.452}$	$-1.731^{+0.496}_{-0.547}$	$-2.639^{+1.144}_{-1.229}$	$1.434^{+0.110}_{-0.106}$	$3.273^{+0.115}_{-0.113}$	0.03
$(0-0.5)$	$\boldsymbol{-0.823^{+0.213}_{-0.216}}$	$-1.188^{+0.210}_{-0.238}$	$\boldsymbol{-1.430^{+0.320}_{-0.370}}$	$-1.603^{+0.416}_{-0.480}$	$-1.734^{+0.492}_{-0.565}$	$-2.642^{+1.050}_{-1.191}$	$1.437^{+0.113}_{-0.104}$	$3.276^{+0.112}_{-0.112}$	0.0
$(0-0.75)$	$\boldsymbol{-0.827^{+0.212}_{-0.206}}$	$-1.178^{+0.230}_{-0.275}$	$-1.412^{+0.338}_{-0.423}$	$\boldsymbol{-1.579^{+0.430}_{-0.541}}$	$-1.704^{+0.503}_{-0.632}$	$-2.582^{+1.042}_{-1.292}$	$1.438^{+0.108}_{-0.108}$	$3.276^{+0.111}_{-0.110}$	-0.003
$(0-1.0)$	$\boldsymbol{-0.822^{+0.209}_{-0.213}}$	$-1.186^{+0.252}_{-0.281}$	$-1.429^{+0.372}_{-0.423}$	$-1.602^{+0.471}_{-0.537}$	$\boldsymbol{-1.732^{+0.548}_{-0.626}}$	$-2.642^{+1.116}_{-1.270}$	$1.436^{+0.108}_{-0.106}$	$3.274^{+0.113}_{-0.111}$	0.02
$(0.25-0.5)$	$-0.827^{+0.604}_{-0.700}$	$\boldsymbol{-1.189^{+0.153}_{-0.177}}$	$\boldsymbol{-1.430^{+0.312}_{-0.362}}$	$-1.602^{+0.546}_{-0.633}$	$-1.731^{+0.728}_{-0.844}$	$-2.635^{+2.022}_{-2.345}$	$1.431^{+0.114}_{-0.105}$	$3.271^{+0.112}_{-0.106}$	0.05
$(0.25-0.75)$	$-0.833^{+0.474}_{-0.557}$	$\boldsymbol{-1.187^{+0.151}_{-0.177}}$	$-1.423^{+0.261}_{-0.308}$	$\boldsymbol{-1.591^{+0.434}_{-0.512}}$	$-1.717^{+0.572}_{-0.674}$	$-2.601^{+1.565}_{-1.846}$	$1.435^{+0.111}_{-0.101}$	$3.277^{+0.111}_{-0.110}$	-0.02
$(0.25-1.0)$	$-0.829^{+0.435}_{-0.512}$	$\boldsymbol{-1.184^{+0.149}_{-0.176}}$	$-1.421^{+0.252}_{-0.297}$	$-1.590^{+0.409}_{-0.482}$	$\boldsymbol{-1.717^{+0.535}_{-0.630}}$	$-2.605^{+1.448}_{-1.705}$	$1.434^{+0.112}_{-0.104}$	$3.273^{+0.112}_{-0.108}$	-0.005
$(0.5-0.75)$	$-0.833^{+2.103}_{-2.509}$	$-1.186^{+0.979}_{-1.168}$	$\boldsymbol{-1.421^{+0.315}_{-0.377}}$	$\boldsymbol{-1.589^{+0.444}_{-0.528}}$	$-1.715^{+0.812}_{-0.966}$	$-2.597^{+3.637}_{-4.333}$	$1.433^{+0.113}_{-0.105}$	$3.278^{+0.111}_{-0.110}$	0.01
$(0.5-1.0)$	$-0.826^{+1.448}_{-1.678}$	$-1.185^{+0.719}_{-0.835}$	$\boldsymbol{-1.424^{+0.318}_{-0.370}}$	$-1.595^{+0.340}_{-0.393}$	$\boldsymbol{-1.723^{+0.545}_{-0.629}}$	$-2.620^{+2.380}_{-2.750}$	$1.437^{+0.110}_{-0.104}$	$3.272^{+0.115}_{-0.110}$	0.02
$(0.75-1.0)$	$-0.820^{+4.644}_{-5.207}$	$-1.184^{+2.629}_{-2.949}$	$-1.427^{+1.304}_{-1.464}$	$\boldsymbol{-1.600^{+0.458}_{-0.516}}$	$\boldsymbol{-1.730^{+0.560}_{-0.625}}$	$-2.640^{+5.509}_{-6.168}$	$1.434^{+0.109}_{-0.106}$	$3.273^{+0.115}_{-0.108}$	-0.004
all	$-0.831^{+0.591}_{-0.650}$	$-1.184^{+0.310}_{-0.324}$	$-1.422^{+0.375}_{-0.373}$	$-1.598^{+0.469}_{-0.471}$	$-1.735^{+0.607}_{-0.607}$	$-2.635^{+1.880}_{-1.847}$	–	–	0.008

Table II. Non-linear EoS test with SNLS3 data: column description is the same of Table. I.

SNLS3	w_0	$w_{0.25}$	$w_{0.5}$	$w_{0.75}$	w_1	w_∞	α	β	$\ln \mathcal{B}_{ij}$
$(0-0.25-0.5)$	$\mathbf{-0.999^{+0.508}_{-0.593}}$	$\mathbf{-1.184^{+0.246}_{-0.245}}$	$\mathbf{-1.640^{+0.475}_{-0.943}}$	$-2.129^{+1.574}_{-2.182}$	$-2.584^{+2.479}_{-3.395}$	$-7.912^{+14.430}_{-14.626}$	$1.434^{+0.114}_{-0.106}$	$3.293^{+0.113}_{-0.111}$	0.43
$(0-0.25-0.75)$	$\mathbf{-0.976^{+0.501}_{-0.576}}$	$\mathbf{-1.179^{+0.248}_{-0.251}}$	$-1.594^{+0.530}_{-0.682}$	$\mathbf{-2.027^{+1.196}_{-2.080}}$	$-2.427^{+1.690}_{-2.222}$	$-7.022^{+9.824}_{-9.952}$	$1.434^{+0.112}_{-0.102}$	$3.286^{+0.117}_{-0.110}$	0.48
$(0-0.25-1.0)$	$\mathbf{-0.952^{+0.489}_{-0.563}}$	$\mathbf{-1.181^{+0.249}_{-0.240}}$	$-1.589^{+0.489}_{-0.588}$	$-2.005^{+1.409}_{-1.787}$	$\mathbf{-2.385^{+1.985}_{-3.193}}$	$-6.686^{+8.037}_{-8.095}$	$1.437^{+0.112}_{-0.108}$	$3.284^{+0.119}_{-0.113}$	0.46
$(0-0.5-0.75)$	$\mathbf{-0.964^{+0.508}_{-0.543}}$	$-1.173^{+0.966}_{-1.518}$	$\mathbf{-1.579^{+0.447}_{-0.829}}$	$\mathbf{-1.999^{+1.187}_{-2.029}}$	$-2.385^{+2.281}_{-3.054}$	$-6.799^{+19.577}_{-23.269}$	$1.434^{+0.111}_{-0.102}$	$3.286^{+0.114}_{-0.108}$	0.42
$*(0-0.5-1.0)$	$\mathbf{-1.169^{+0.595}_{-0.618}}$	$-1.297^{+0.608}_{-1.013}$	$\mathbf{-1.848^{+0.629}_{-1.129}}$	$-1.810^{+0.588}_{-0.834}$	$\mathbf{-3.654^{+2.850}_{-4.132}}$	$-3.709^{+9.653}_{-11.524}$	$1.436^{+0.109}_{-0.105}$	$3.295^{+0.116}_{-0.111}$	0.63
$*(0-0.75-1.0)$	$\mathbf{-0.983^{+0.513}_{-0.553}}$	$-1.150^{+2.835}_{-4.827}$	$-1.549^{+2.388}_{-4.223}$	$\mathbf{-1.974^{+1.129}_{-2.142}}$	$\mathbf{-2.370^{+1.901}_{-3.443}}$	$-6.989^{+28.761}_{-41.367}$	$1.438^{+0.109}_{-0.105}$	$3.286^{+0.115}_{-0.111}$	0.39
$(0.25-0.5-0.75)$	$-1.033^{+4.544}_{-6.938}$	$\mathbf{-1.168^{+0.252}_{-0.252}}$	$\mathbf{-1.560^{+0.430}_{-0.788}}$	$\mathbf{-1.988^{+1.155}_{-1.967}}$	$-2.390^{+2.575}_{-3.486}$	$-7.146^{+30.706}_{-44.669}$	$1.434^{+0.111}_{-0.100}$	$3.287^{+0.118}_{-0.111}$	0.49
$*(0.25-0.5-1.0)$	$-0.852^{+2.846}_{-4.810}$	$\mathbf{-1.184^{+0.245}_{-0.240}}$	$\mathbf{-1.538^{+0.433}_{-0.876}}$	$-1.856^{+0.671}_{-1.058}$	$\mathbf{-2.130^{+1.834}_{-3.712}}$	$-4.903^{+16.540}_{-25.980}$	$1.435^{+0.113}_{-0.104}$	$3.283^{+0.116}_{-0.111}$	0.41
$(0.25-0.75-1.0)$	$-1.063^{+9.101}_{-13.230}$	$\mathbf{-1.175^{+0.245}_{-0.246}}$	$-1.567^{+1.789}_{-2.706}$	$\mathbf{-2.003^{+1.163}_{-1.842}}$	$\mathbf{-2.415^{+1.969}_{-2.947}}$	$-7.342^{+41.340}_{-58.128}$	$1.432^{+0.112}_{-0.102}$	$3.284^{+0.114}_{-0.107}$	0.47
$(0.5-0.75-1.0)$	$-1.100^{+31.507}_{-43.681}$	$-1.204^{+7.430}_{-10.429}$	$\mathbf{-1.505^{+0.393}_{-0.629}}$	$\mathbf{-1.834^{+1.078}_{-1.567}}$	$\mathbf{-2.143^{+1.854}_{-2.514}}$	$-5.800^{+68.838}_{-92.726}$	$1.434^{+0.110}_{-0.106}$	$3.280^{+0.116}_{-0.110}$	0.38
all $(2NL)$	$-1.014^{+2.155}_{-2.438}$	$-1.180^{+0.635}_{-0.627}$	$-1.604^{+0.865}_{-0.904}$	$-2.036^{+1.505}_{-1.578}$	$-2.451^{+2.685}_{-2.717}$	$-7.492^{+33.305}_{-34.154}$	–	–	0.46
$(0-0.25-0.5-0.75)$	$\mathbf{-1.604^{+0.875}_{-0.993}}$	$\mathbf{-1.299^{+0.300}_{-0.309}}$	$\mathbf{-2.091^{+0.664}_{-0.908}}$	$\mathbf{-1.299^{+1.193}_{-2.109}}$	$-0.744^{+3.626}_{-6.110}$	$87.490^{+101.156}_{-156.963}$	$1.436^{+0.110}_{-0.103}$	$3.303^{+0.113}_{-0.113}$	0.35
$(0-0.25-0.5-1.0)$	$\mathbf{-1.568^{+0.906}_{-0.996}}$	$\mathbf{-1.317^{+0.293}_{-0.340}}$	$\mathbf{-2.045^{+0.685}_{-0.944}}$	$-1.310^{+1.577}_{-1.901}$	$\mathbf{0.576^{+3.841}_{-4.484}}$	$80.387^{+91.018}_{-109.622}$	$1.436^{+0.112}_{-0.107}$	$3.303^{+0.114}_{-0.114}$	0.37
$*(0-0.25-0.75-1.0)$	$\mathbf{-1.384^{+0.904}_{-0.885}}$	$\mathbf{-1.201^{+0.309}_{-0.316}}$	$-1.821^{+2.574}_{-8.153}$	$\mathbf{-2.155^{+1.667}_{-6.167}}$	$\mathbf{-2.164^{+4.730}_{-12.359}}$	$13.224^{+223.327}_{-634.365}$	$1.437^{+0.112}_{-0.108}$	$3.284^{+0.119}_{-0.113}$	0.56
$(0-0.5-0.75-1.0)$	$\mathbf{-1.589^{+0.856}_{-0.903}}$	$-1.466^{+0.623}_{-0.900}$	$\mathbf{-2.034^{+0.623}_{-0.900}}$	$\mathbf{-1.175^{+1.004}_{-1.864}}$	$\mathbf{0.767^{+3.055}_{-4.616}}$	$77.831^{+229.220}_{-367.508}$	$1.434^{+0.112}_{-0.105}$	$3.303^{+0.114}_{-0.112}$	0.25
$(0.25-0.5-0.75-1.0)$	$17.219^{+38.421}_{-62.723}$	$\mathbf{-1.328^{+0.294}_{-0.301}}$	$\mathbf{-2.132^{+0.637}_{-0.847}}$	$\mathbf{-1.129^{+1.114}_{-2.076}}$	$\mathbf{-1.078^{+3.387}_{-5.091}}$	$-100.955^{+353.279}_{-569.121}$	$1.435^{+0.110}_{-0.105}$	$3.303^{+0.117}_{-0.110}$	0.34
all $(3NL)$	$-1.436^{+1.559}_{-1.167}$	$-1.301^{+0.492}_{-0.489}$	$-2.063^{+0.997}_{-0.930}$	$-1.388^{+1.580}_{-1.653}$	$-0.252^{+4.424}_{-4.623}$	$62.123^{+194.079}_{-254.463}$	–	–	0.37

Table III. Linear EoS test with Union2.1 data: column description is the same of Table. I.

Union2.1	w_0	$w_{0.25}$	$w_{0.5}$	$w_{0.75}$	w_1	w_∞
CPL	$\mathbf{-0.933^{+0.231}_{-0.224}}$	$-0.907^{+0.327}_{-0.344}$	$-0.890^{+0.475}_{-0.512}$	$-0.877^{+0.592}_{-0.642}$	$-0.868^{+0.683}_{-0.743}$	$\mathbf{-0.803^{+1.347}_{-1.469}}$
$(0-0.25)$	$\mathbf{-0.972^{+0.246}_{-0.246}}$	$\mathbf{-0.912^{+0.105}_{-0.113}}$	$-0.872^{+0.239}_{-0.250}$	$-0.843^{+0.360}_{-0.371}$	$-0.822^{+0.453}_{-0.465}$	$-0.672^{+1.115}_{-1.135}$
$(0-0.5)$	$\mathbf{-0.967^{+0.245}_{-0.247}}$	$-0.915^{+0.167}_{-0.171}$	$\mathbf{-0.880^{+0.225}_{-0.233}}$	$-0.855^{+0.298}_{-0.308}$	$-0.836^{+0.359}_{-0.371}$	$-0.706^{+0.834}_{-0.856}$
$(0-0.75)$	$\mathbf{-0.968^{+0.244}_{-0.252}}$	$-0.912^{+0.204}_{-0.215}$	$-0.875^{+0.268}_{-0.286}$	$\mathbf{-0.848^{+0.337}_{-0.360}}$	$-0.828^{+0.395}_{-0.422}$	$-0.688^{+0.851}_{-0.905}$
$(0-1.0)$	$\mathbf{-0.968^{+0.244}_{-0.249}}$	$-0.913^{+0.225}_{-0.233}$	$-0.876^{+0.297}_{-0.309}$	$-0.850^{+0.369}_{-0.384}$	$\mathbf{-0.830^{+0.428}_{-0.446}}$	$-0.692^{+0.890}_{-0.926}$
$(0.25-0.5)$	$-0.988^{+0.413}_{-0.448}$	$\mathbf{-0.911^{+0.102}_{-0.110}}$	$\mathbf{-0.860^{+0.217}_{-0.236}}$	$-0.824^{+0.379}_{-0.412}$	$-0.796^{+0.505}_{-0.548}$	$-0.605^{+1.398}_{-1.519}$
$(0.25-0.75)$	$-0.972^{+0.357}_{-0.378}$	$\mathbf{-0.913^{+0.105}_{-0.111}}$	$-0.874^{+0.203}_{-0.215}$	$\mathbf{-0.846^{+0.340}_{-0.360}}$	$-0.825^{+0.447}_{-0.474}$	$-0.679^{+1.219}_{-1.290}$
$(0.25-1.0)$	$-0.966^{+0.329}_{-0.341}$	$\mathbf{-0.911^{+0.100}_{-0.111}}$	$-0.874^{+0.197}_{-0.201}$	$-0.848^{+0.325}_{-0.329}$	$\mathbf{-0.828^{+0.426}_{-0.431}}$	$-0.690^{+1.148}_{-1.164}$
$(0.5-0.75)$	$-0.969^{+1.540}_{-1.654}$	$-0.912^{+0.710}_{-0.763}$	$\mathbf{-0.874^{+0.222}_{-0.240}}$	$\mathbf{-0.847^{+0.335}_{-0.357}}$	$-0.827^{+0.609}_{-0.652}$	$-0.685^{+2.697}_{-2.890}$
$(0.5-1.0)$	$-0.961^{+1.071}_{-1.151}$	$-0.909^{+0.519}_{-0.563}$	$\mathbf{-0.875^{+0.218}_{-0.241}}$	$-0.850^{+0.260}_{-0.276}$	$\mathbf{-0.832^{+0.424}_{-0.448}}$	$-0.703^{+1.818}_{-1.932}$
$(0.75-1.0)$	$-0.954^{+3.505}_{-3.672}$	$-0.906^{+1.979}_{-2.074}$	$-0.875^{+0.976}_{-1.025}$	$\mathbf{-0.852^{+0.338}_{-0.357}}$	$\mathbf{-0.835^{+0.431}_{-0.448}}$	$-0.716^{+4.182}_{-4.369}$
all	$-0.963^{+0.483}_{-0.483}$	$-0.912^{+0.228}_{-0.238}$	$-0.877^{+0.268}_{-0.261}$	$-0.840^{+0.336}_{-0.348}$	$-0.832^{+0.467}_{-0.451}$	$-0.687^{+1.432}_{-1.404}$